Snow crystal imaging using scanning electron microscopy: III. Glacier ice, snow and biota

A. RANGO
USDA Hydrology Laboratory, Agricultural Research Service, Beltsville, Maryland 20705, USA
e-mail: alrango@hydrolab.arsusda.gov

W. P. WERGIN, E. F. ERBE
USDA Nematology Laboratory, Agricultural Research Service, Beltsville, Maryland 20705, USA

E. G. JOSBERGER
US Geological Survey, 1201 Pacific Ave, Suite 600, Tacoma, Washington 98416, USA

Abstract Low-temperature scanning electron microscopy (SEM) was used to observe metamorphosed snow, glacial firn, and glacial ice obtained from South Cascade Glacier in Washington State, USA. Biotic samples consisting of algae (*Chlamydomonas nivalis*) and ice worms (a species of oligochaetes) were also collected and imaged. In the field, the snow and biological samples were mounted on copper plates, cooled in liquid nitrogen, and stored in dry shipping containers which maintain a temperature of –196°C. The firn and glacier ice samples were obtained by extracting horizontal ice cores, 8 mm in diameter, at different levels from larger standard glaciological (vertical) ice cores 7.5 cm in diameter. These samples were cooled in liquid nitrogen and placed in cryotubes, were stored in the same dry shipping container, and sent to the SEM facility. In the laboratory, the samples were sputter coated with platinum and imaged by a low-temperature SEM. To image the firn and glacier ice samples, the cores were fractured in liquid nitrogen, attached to a specimen holder, and then imaged. While light microscope images of snow and ice are difficult to interpret because of internal reflection and refraction, the SEM images provide a clear and unique view of the surface of the samples because they are generated from electrons emitted or reflected only from the surface of the sample. In addition, the SEM has a great depth of field with a wide range of magnifying capabilities. The resulting images clearly show the individual grains of the seasonal snowpack and the bonding between the snow grains. Images of firn show individual ice crystals, the bonding between the crystals, and connected air spaces. Images of glacier ice show a crystal structure on a scale of 1–2 mm which is considerably smaller than the expected crystal size. Microscopic air bubbles, less than 15 μm in diameter, clearly marked the boundaries between these crystal-like features. The life forms associated with the glacier were easily imaged and studied. The low-temperature SEM sample collecting and handling methods proved to be operable in the field; the SEM analysis is applicable to glaciological studies and reveals details unattainable by conventional light microscopic methods.

Imagerie des cristaux de glace par microscopie électronique à balayage: III. Glace de glacier, neige, matière vivante

Résumé La microscopie électronique à balayage à basse température a été utilisée pour observer de la neige transformée, de la glace de névé et de la glace de glacier du glacier "South Cascade" (Washington, Etats-Unis). Des algues (*Chlamydomonas nivalis*) et des vers de glace (une espèce d'oligochètes) ont également été recueillis et observés. Sur le terrain, les échantillons biologiques et de neige ont été montés sur des plaques de cuivre, refroidis dans l'azote liquide et stockés dans des conteneurs de transport secs maintenant la température à –196°C. Les échantillons de glace de névé et de glacier ont été obtenus par extraction de carottes de glace horizontales de 8 mm de diamètre à différents niveaux de carottes de glace verticales de 7.5 cm de diamètre. Ces échantillons ont été refroidis dans l'azote liquide et placés dans des cryotubes eux

mêmes stockés dans les mêmes conteneurs que les précédents échantillons. Au laboratoire, les échantillons ont été recouverts de platine par pulvérisation et observés par un microscope électronique à balayage à basse température. Pour observer les échantillons de glace de névé et de glacier, les carottes ont été fracturées dans l'azote liquide puis placées sur un support avant d'être photographiées. Alors que les images de la neige et de la glace obtenues par microscopie optique sont difficiles à interpréter en raison de réflexions et réfractions internes, les images de microscopie électronique à balayage fournissent des vues claires et nettes de la surface des échantillons, parce qu'elles proviennent des seuls électrons émis ou réfléchis par la surface de l'échantillon. De plus la microscopie électronique à balayage offre une grande profondeur de champ et toute une gamme d'agrandissements. Les images obtenues montrent clairement chaque grain de la couche de neige saisonnière et les liaisons entre grains de neige. Les images de névés montrent les cristaux de neige individuels, les liaisons entre les cristaux et des poches d'air interconnectées. Les images de glace de glacier présentent une structure cristalline à l'échelle de 1 ou 2 mm qui est considérablement plus petite que la taille attendue des cristaux. Des bulles d'air microscopiques, d'un diamètre inférieur à 15 μm, marquent très nettement les frontières entres ces structures d'allure cristalline. Les formes de vie associées au glacier ont pu être facilement photographiées et étudiées. La collecte et la manipulation des échantillons destinés à la microscopie électronique à balayage à basse température s'est révélée réalisable sur le terrain; la microscopie électronique à balayage est applicable aux études glaciologiques et révèle des détails qu'il serait impossible d'obtenir par les méthodes classiques de microscopie optique.

INTRODUCTION

Snow can cover up to 53% of the land surface in the northern hemisphere (Foster & Rango, 1982) and up to 44% of the global land area at any one time (Rango *et al.*, 1996a). Ice, in the form of glaciers, covers just 10% of the land area (Hall & Martinec, 1985) and is usually covered by snow. However, these glaciers contain 75% of the Earth's freshwater supply (Hall & Martinec, 1985). They are economically important as sources of freshwater and for the generation of hydroelectric power in areas of Norway, Iceland, Alaska, the northwestern United States, western Canada, Asia, and the European Alps. In individual river basins, where glaciers cover a large percentage of the drainage area, a large proportion of the total streamflow is derived from glacier melt.

The real hydrological impact of glaciers, however, is not so much their contribution to the total streamflow, but rather their timely release of water during dry periods (Richardson, 1972). Glacier-dominated streams reach their maximum streamflow during the warmest summer months (July and August in the northern hemisphere) as opposed to snowmelt dominated streams where peak flows usually occur in May and June. In Scandinavia, for example, glaciers release almost 85% of their total annual discharge during July–September (Ostrem, 1972). In addition to their effect on time of seasonal peak flow, glaciers that are growing (positive mass balance) or decreasing (negative mass balance) will restrict or enhance the natural streamflow, respectively. Hence, they act as natural reservoirs, storing water in cool wet years and releasing water during warm dry years. During certain years, a glacier may affect the basin water yield by as much as ±20–30% (Ostrem, 1972).

In the high elevation river basins of the Tien Shan Mountains in Asia, glaciers can cover up to 50% of a drainage basin. In basins where glaciers cover at least 30–40% of the area, the average contribution of glacier runoff is 18–24% of the average annual runoff (increasing to as much as 40–70% in summer) (Aizen *et al.*, 1996). In contrast, rain contributes 7–12% of annual runoff volume, seasonal snowmelt about 18%, and groundwater 36–38% while 10% of the average annual runoff is lost during channel

transit in the basin (Aizen *et al.*, 1996). As the surface area covered by glaciers diminishes, the contribution of snowmelt increases in a compensating manner.

Understanding glaciers is valuable for reasons other than the hydrological impacts. Glaciers and their fluctuations in extent and volume are indicators of climate change, past and present. Additionally, the microscopic ice crystal structure can reveal information on past climate conditions. For example, entrapped air bubbles, impurities in the ice, and chemical constituents all contain information about conditions under which the ice originally accumulated and on significant events occurring during the life history of the glacier. The size and shape of ice crystals in a vertical profile from the surface of the glacier down to 10–20 m depth provides information on the metamorphosis of snow and ice in recent times. The presence, location, and orientation of air bubbles also provide information on the metamorphosis of the snow to glacier ice. Recently developed techniques in low temperature scanning electron microscopy (SEM) of snow crystals are used to image a variety of samples from a mountain glacier to evaluate and demonstrate this technique for observing a variety of glacier ice types.

The general techniques of low temperature scanning electron microscopy, described by Rango *et al.* (1996a,b) for collecting and imaging precipitated and metamorphosed snow crystals, were used for this study of glacier snow, ice and biota. However, new methods had to be developed to obtain the samples from the glacier and to mount ice core samples in the SEM. Transport of the samples to the SEM facility remained the same except that the remote location of this site required a helicopter to access the site. To test the methodology and evaluate its potential for glacier studies, snow and ice and biotic materials were sampled from the South Cascade Glacier in the Cascade Mountains of Washington state in August 1996.

BACKGROUND

Samples of glacier snow and ice have been previously imprinted and photographed by several methods (Ahlmann & Droessler 1949; Seligman 1949; Eckerbom & Palosuo 1963). In a procedure developed by Ahlmann & Droessler (1949), individual crystals were photographed by spreading dyes, which were non-soluble in water, on the smooth ice surface. Next, paper was gently pressed onto the surface of the crystals to create an imprint that could be photographed. The use of imprints was limited to relatively smooth surfaces and prevented observations of magnified crystals. However, this technique did provide structural information about the external surface as opposed to direct observations of crystals by light microscopy in which the internal and external structural features were combined in a single image.

The application of low temperature SEM for observation of snow crystals has been previously demonstrated by the Electron Microscope Unit of USDA in Beltsville, Maryland (Wergin & Erbe 1994a,b,c; Wergin *et al.* 1995a,b, 1996). Recently, Wergin *et al.* (1998) demonstrated that the same procedure has application to the study of ice cores. For ice core studies using visible light photography, the final image has a greatly limited depth of field and contains a mixture of information that results from reflected, refracted and transmitted light, regardless of how the ice specimen was illuminated for observation and photographed (with a video or light microscope). As a result, interpreting the surface features of the specimen is frequently confounded by subsurface structure, which also contributes to the final image. A SEM image only

provides information on structure of the surface because it results from electrons back scattered from the surface of the specimen and secondary electrons emanating from the surface of the sample. Hence, surface features, such as ice crystal boundaries and bubble size and orientation, are distinctly discerned.

STUDY SITE

Samples of glacier snow, ice, and biota were obtained from South Cascade Glacier, a valley glacier of 2.5 km^2 area on the western slope of the main divide of the North Cascades in north central Washington state, USA. Figure 1 shows the location of the glacier in Washington state and a detailed schematic diagram of the glacier and its features. Figure 2 is an aerial oblique view of the glacier. The topography in this immediate area, which is extremely rugged, requires the use of a helicopter for rapid access to the glacier. The present maritime climate of the region supports more than 700 glaciers (Post *et al.*, 1971) through heavy winter precipitation. On South Cascade

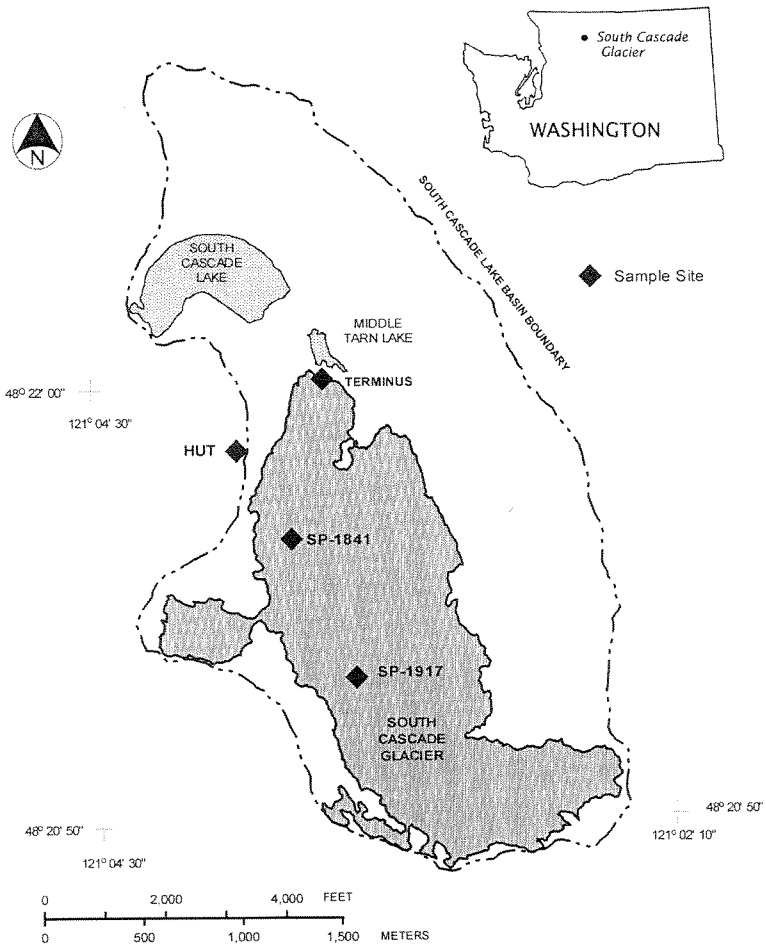

Fig. 1 Map of South Cascade Glacier and vicinity.

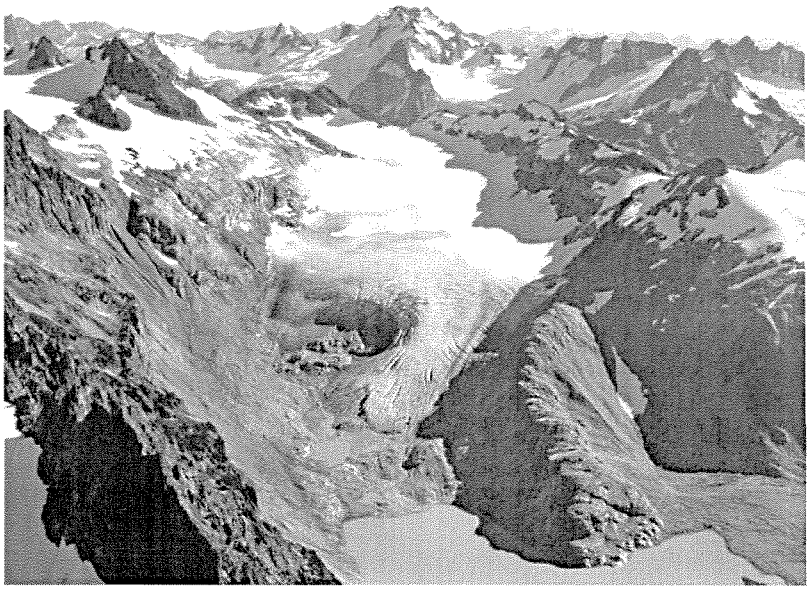

Fig. 2 Low-altitude oblique view looking southeast toward the USGS research hut and the South Cascade Glacier.

Glacier, the annual precipitation can exceed 4.5 m of snow water equivalent, most of that falling as snow from October to May (Meier *et al.*, 1971; Krimmel, 1996). The equilibrium line, the elevation where winter snow accumulation equals summer ablation, lies at approximately 1900 m. The basin containing the glacier is in a small north-facing valley 6.1 km^2 in area. Runoff from the glacier enters the South Fork Cascade River, a tributary of the Skagit River which discharges into Puget Sound 100 km into the west.

South Cascade Glacier is part of the continuing US Geological Survey Benchmark Glacier Programme. As part of this programme, detailed mass-balance observations have been made on this glacier every year since the International Geophysical Year in 1959 (Krimmel, 1996). Hodge *et al.* (1998) described these measurements and the links between recent climatic shifts and mass balance. Furthermore this glacier has been the subject of extensive study over the past 40 years which greatly aided the interpretation of the SEM images.

MATERIALS AND METHODS

Samples of snow, glacier ice, and associated biota were acquired on 6 August 1996 at 4 locations on or near South Cascade Glacier. These sites are shown by the symbol ◆ in Fig. 1. Snow samples containing high concentrations of algae, commonly know "red" snow, were acquired from snow fields 100 and 150 m south of the USGS research hut which is located on a narrow ridge immediately west of the glacier at an elevation of 1848 m. Surface melting concentrates the algae to very high levels, giving the snow a pinkish colour at the bottom of runnels, small valley-like depressions in the

snow surface, typically 1 m across and 0.2 m deep. These snow samples were placed directly onto copper plates (16 × 30 mm and 1.5 mm thick) that were pre-cooled to 0°C. The sample holders were plunged into liquid nitrogen, transferred to square brass tubes pre-cooled with liquid nitrogen to –196°C and placed in an insulated dry shipper at –196°C for storage and subsequent shipping to the laboratory at Beltsville, Maryland. Samples of snow grains from beneath the surface layer of "red" snow were also acquired.

Samples of snow and glacier ice were obtained from two sites on the glacier which are labelled in Fig. 1 as SP-1841 and SP-1917, according to their elevation in metres. An ice coring auger with a 7.5 cm diameter core was used to obtain samples of the seasonal snow and glacier ice below. At the lower site, SP-1841, the auger was used to extract a 2.25 m core that was 7.5 cm in diameter. The core consisted of 1.88 m of snow on top of a hard horizon of "dirty" ice that was approximately 2 cm thick. Below this dirty layer was a 5 cm thick layer of very bubbly ice followed by 30 cm of ice with much smaller bubbles. At the upper site, SP-1917, a 3.25 m sample core was obtained with a snow depth of 3.0 m on top of 25 cm of what appeared to be firn or glacier ice. As at the lower site, the ice portion of the core contained a 5-cm thick layer of bubbly ice on top of ice that was much less bubbly, but there was no "dirty" ice layer.

Snow crystal samples for SEM analysis were obtained by gently adhering the snow crystals to a pre-cooled layer of methyl cellulose solution coating the copper plates, which were then rapidly cooled and stored in liquid nitrogen (–196°C). A different technique was used to sample the hard firn or ice that was obtained by coring. The ice samples for SEM analysis were obtained by taking cores 8 mm in diameter, perpendicular to the longitudinal axis of the main cylindrical core. These secondary cores were taken every 50–100 mm with a small cork borer (cooled in liquid nitrogen) that had been modified by filing teeth into the cutting edge. The 8 mm diameter cores were plunged in liquid nitrogen, placed in 8 ml cryotubes, and stored in the dry shipper (at –196°C) for transport to Beltsville, Maryland for imaging and analysis. A block of ice obtained from the glacier terminus near Middle Tarn provided the oldest ice sample. This ice was "dirty" as it contained fine-grained bedrock material; the terminus ice was sampled using the cork borer described previously.

Although ice worms (a species of oligochaetes) were not evident in the snow on the glacier surface, they did appear in abundance under an insulating pad that was used for kneeling in the bottom of a 1.0 m deep snow pit at site SP-1841. The worms were dark brown and black and moved rapidly among the snow grains. Individual worms were selected and placed on cooled copper metal plates, plunge frozen in liquid nitrogen, and stored for shipping.

After the dry shipper was received in Beltsville, the frozen samples were transferred to a large storage Dewar for storage and future analysis. For SEM analysis, the copper metal sample plates were removed from this Dewar, placed in specimen holders, and transferred to the preparation chamber of an Oxford CT 1500 HF Cryotrans System for sputter coating with platinum (Pt). Samples were then placed on the pre-cooled (–185°C) stage of a Hitachi S-4100 field emission scanning electron microscope (SEM) where they were imaged and photographed.

In the SEM laboratory, the snow and biotic samples were treated like metamorphosed snow crystals, previously described by Rango *et al.* (1996b), but the ice cores had to be specially mounted for imaging. When the 8 mm ice cores were

removed from the storage Dewar, they were freshly fractured in liquid nitrogen, mounted on a modified copper plate with methyl cellulose solution, and replunged in liquid nitrogen. These sample plates were then transferred to the cryochamber, coated as above, and imaged in the SEM. In some cases, complementary halves of the fractured core were mounted side by side for comparison. In other cases, SEM and light microscope images were taken of the same sample for comparison. Many of the images presented here are composites of multiple (up to 10) single images because the samples and many of the features are much larger than the field of view generally imaged by a SEM. An image processor (Photoshop) was used to produce single seamless images. Additionally, many samples were tilted to produce images that could be viewed in stereo.

RESULTS

As with snowpacks on the ground, the processes by which new snow crystals are transformed after they fall on the surface of a glacier can be rapid and dramatic. Similar to processes in a seasonal snowpack, the fine structure of the new snow crystals is lost in favour of rounded grains (Rango *et al.*, 1996b). Figure 3 shows some rounded snow grains from SP-1841 (at 10 cm below the snow surface) that illustrate the effects of summer melting. The grains are well rounded, range in diameter from 0.5–1.25 mm, and are connected by necks that resulted from freeze-thaw cycling. While some of the ice may have been liquid water at the time of sampling and was subsequently frozen in the sampling process, it is unlikely that the overall structure was greatly modified. The snow at the time of sampling was not remarkably wet and Rango *et al.* (1996b) observed similar features in snow that was subject to freeze-thaw cycling. Figure 4 shows a snow sample from the core taken at site SP-1917, from a depth of approximately 2.5 m. It shows a high degree of necking between the snow grains, and the snow grains are somewhat larger than observed at SP 1841.

Fig. 3 Rounded snow grains from 10 cm below the snow surface at site SP-1841.

Fig. 4 Rounded snow grains from 2.5 m below the snow surface at site SP-1917.

Figure 5 is a composite image of the fractured cross section of an 8 mm core (from the small cork borer) of the ice from the "dirty" ice layer approximately 1 cm below the bottom of the seasonal snowpack at site SP-1841. The hardness, distinct ice grains, and interconnected air volumes indicate that this likely is firn deposited in the 1990–

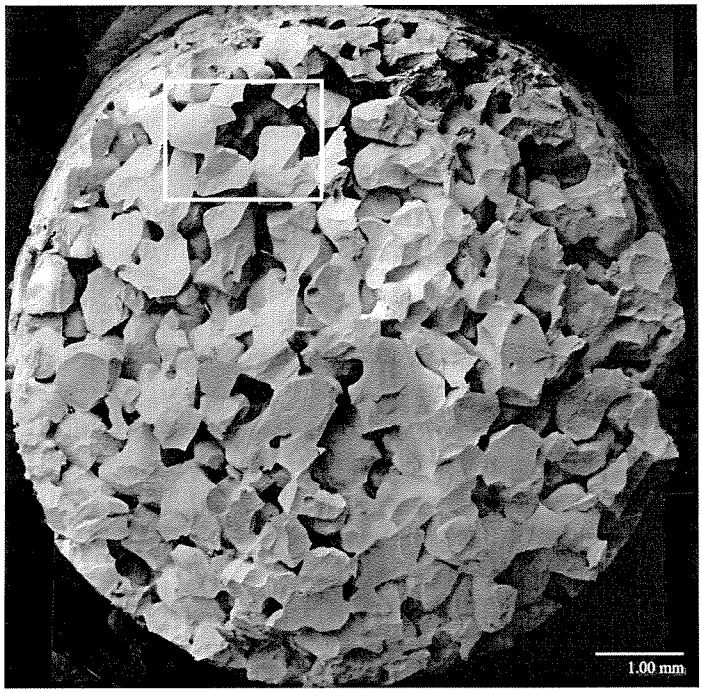

Fig. 5 SEM micrograph composite of a core sample of firn from the dirty ice layer at site SP-1841. Enlargements of the area within the rectangular box are shown in Fig. 6.

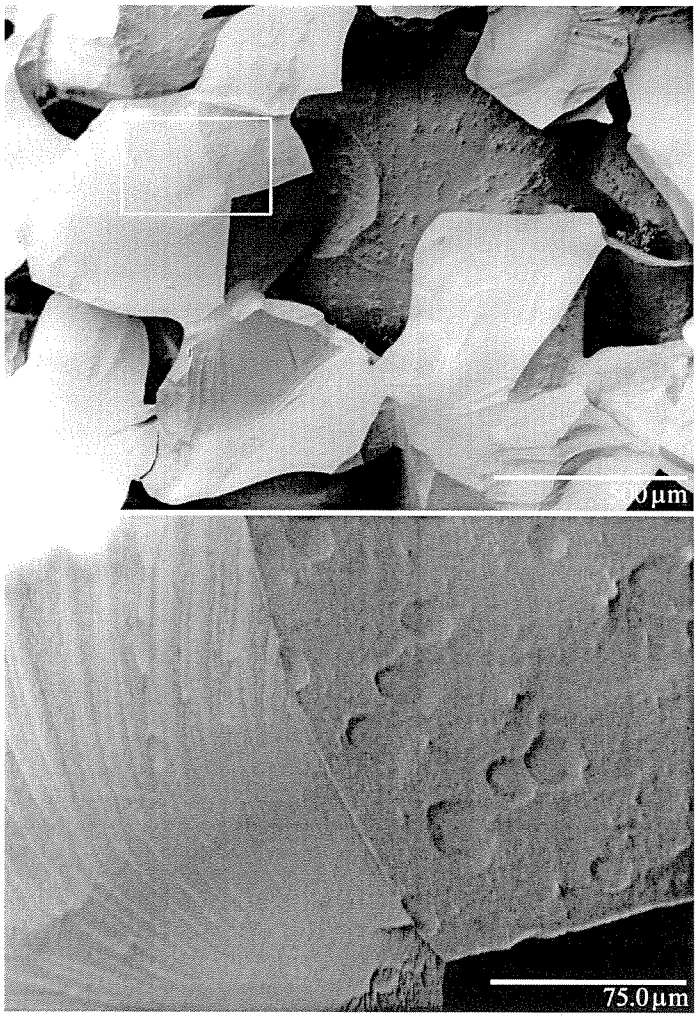

Fig. 6 Two-step enlargements of the rectangular box in Fig. 5.

1991 period, which was the most recent accumulation event at this location on the glacier. The long term USGS measurements at South Cascade glacier provided the information necessary to approximately date the ice samples, which will be discussed later. The rectangle in the upper left portion of Fig. 5 was enlarged to demonstrate the magnification capabilities of the SEM. Figure 6 includes the enlargement of the rectangle in Fig. 5 and a further enlargement of the rectangle in the upper panel of Fig. 6. The first enlargement shows several distinct grains, grain boundaries and the interconnected air spaces typical of firn. The glaciological definition of firn is snow that has lasted through one or more melt seasons and the air volumes within the snow are still in connected with each other. The second enlargement, the lower panel of Fig. 6, is an enlargement of a grain boundary.

Figure 7 is a composite image of a fractured 8 mm core cross section from a depth of 33 cm below the seasonal snowpack at site SP-1841. When compared to the ice in

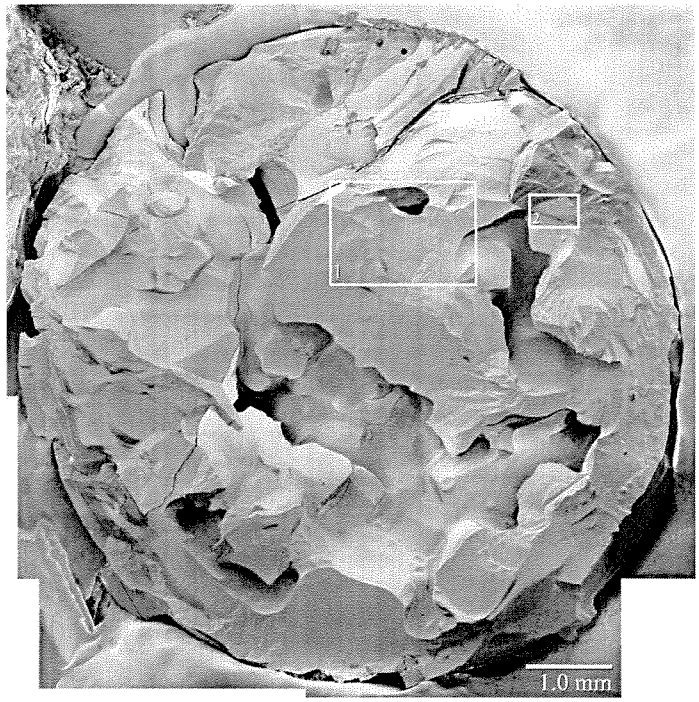

Fig. 7 SEM micrograph composite of core sample from 33 cm below seasonal snow layer from site SP-1841.

Fig. 5, there is a striking difference: the voids depicted in Fig. 7 are larger but appear to have less connectivity; the ice in Fig. 7 is more amorphous and the individual grains are less distinct. Figure 8, which is a two-part enlargement of box 1 in Fig. 7 and comparable to Fig. 6, more clearly defines the individual grain boundaries, which are delineated by microscopic air bubbles. The ice grains are about 2 mm in diameter, whereas the air bubbles are 15 μm or less in diameter. Figure 9 is another two-part enlargement from Fig. 7 (box 2) which shows ice with air bubbles (again less than 15 μm in diameter) in an interesting near-linear alignment pattern as well as repetitive surface facets within each bubble.

To establish the approximate age of the ice samples obtained at SP-1841 and SP-1917, the position of the equilibrium, or firn line on the glacier at the end of the summer for the years 1990–1995 was examined. The USGS observations for 1992–1995 by Krimmel (1993, 1994, 1995, 1996 and personal communication 1990, 1991), show that the firn line location was below the two sample sites for 1990 and 1991 and well above these sites for the other years. Hence, the ice samples from the bottom of the cores could only be from metamorphosed snow that was deposited in the winter of 1991 or earlier.

The ice shown in Fig. 7 is likely much older than that shown in Fig. 5 because it was from a layer below the ice in Fig. 5 and shows a much higher degree of metamorphism. Inspection of the 35-year-long record of mass balance observations at South Cascade can provide some information on its age. As described previously, it must be older than the 1990–1991 period. Field observations and the mass balance

Fig. 8 Two-step enlargements of rectangular box 1 in Fig. 7 showing ice grain boundaries and air volumes.

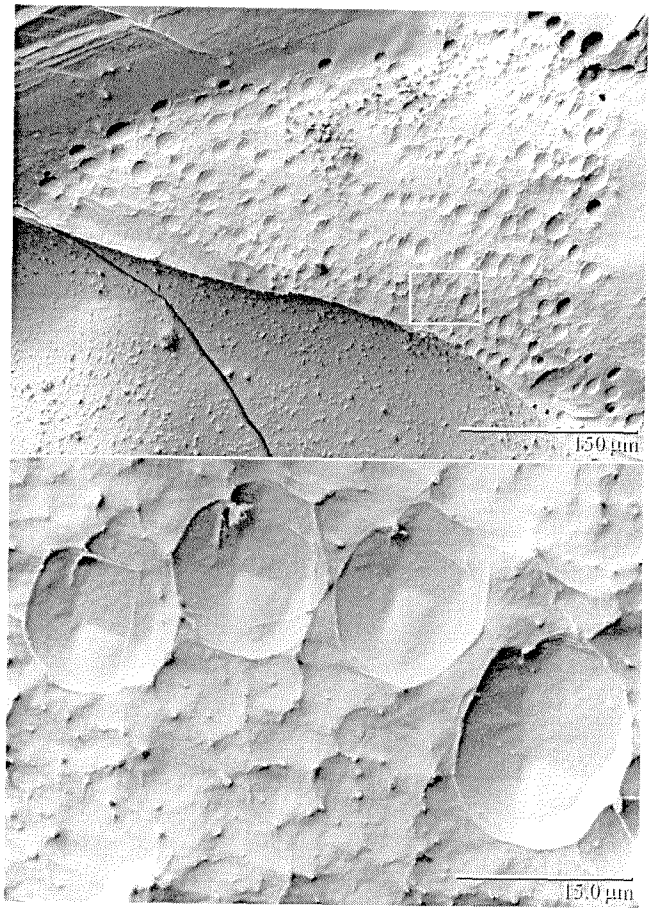

Fig. 9 Two-step enlargements of rectangular box 2 in Fig. 7 showing ice grain boundaries and air volumes.

measurements prior to this period show that there were four different years with very negative mass balances that removed considerable mass from the surface of the glacier, including large amounts of firn. Hodge *et al.* (1998) showed that these years were 1977, 1979, 1987, and 1988, and field observations from 1989 to 1997 show that there was no accumulation at the altitude of either of the two sites. Therefore, the ice in Fig. 7 is probably the result of accumulation prior to 1977, a period when the mass balance was consistently near zero. It is unlikely that glacier flow brought newer firn from higher on the glacier into this area because the flow rates are typically 10 m $year^{-1}$, which for a period of approximately 20 years gives a displacement of only 200 m. No further attempt was made to precisely date these samples because the intent of this study was to demonstrate the unique capabilities of low temperature SEM for imaging glacier snow and ice types.

A sample of ice at the terminus of the glacier, broken off with an ice axe, provided older glacier ice for SEM imaging. Given a typical flow rate of 10 m $year^{-1}$ and a length of 2.5 km to the main accumulation area of the glacier, an approximate age of 250 years can be estimated for this sample. Figure 10 shows a composite SEM image of a fractured 8 mm core cross section extracted from the larger terminus sample; the hardness of the ice made it difficult to obtain a perfectly circular core. The individual ice grains are not immediately evident and the air voids are smaller and less numerous than in the samples from higher on the glacier (Figs 5 and 7). Magnification of boxes 1 and 2 of Fig. 10 further illustrate the capabilities of the SEM for imaging glacier ice. Figure 11 is a two-step enlargement of an elongated air bubble within box 1 of Fig. 10.

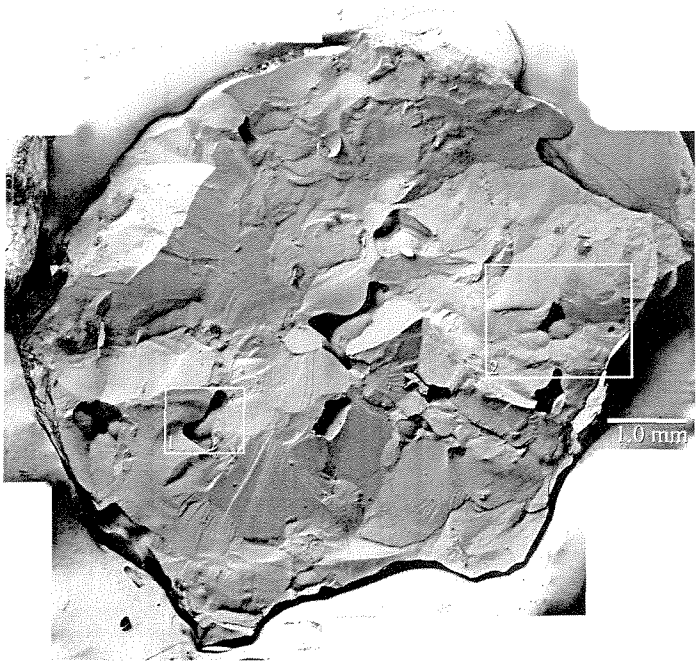

Fig. 10 SEM micrograph composite of core sample of old glacier ice obtained at the terminus of the South Cascade Glacier near Middle Tarn Lake. Box 1 shows an elongated air bubble approximately 1 mm long. Box 2 marks an area of numerous grain boundaries that are denoted by microscopic bubbles.

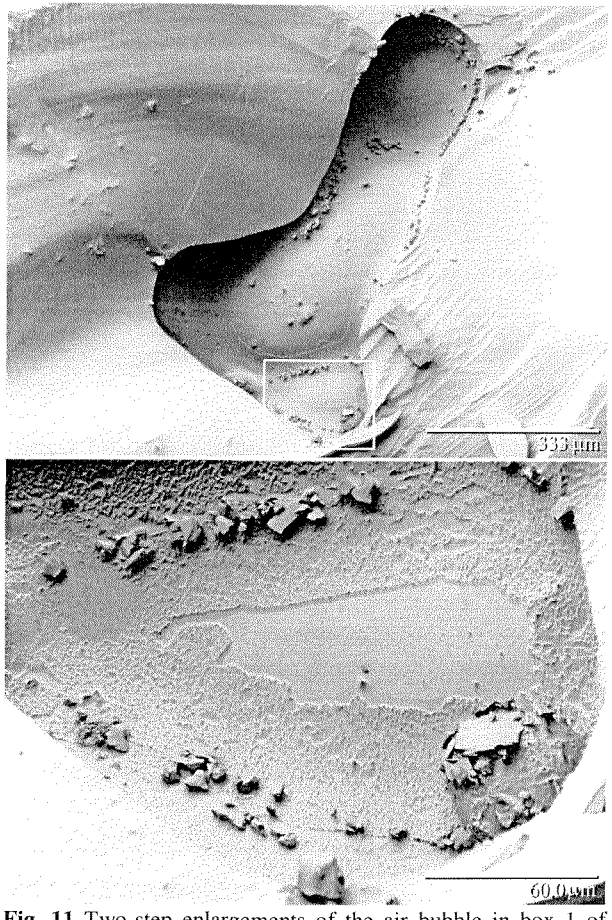

Fig. 11 Two-step enlargements of the air bubble in box 1 of Fig. 10, which shows particulate matter on the walls of the bubble.

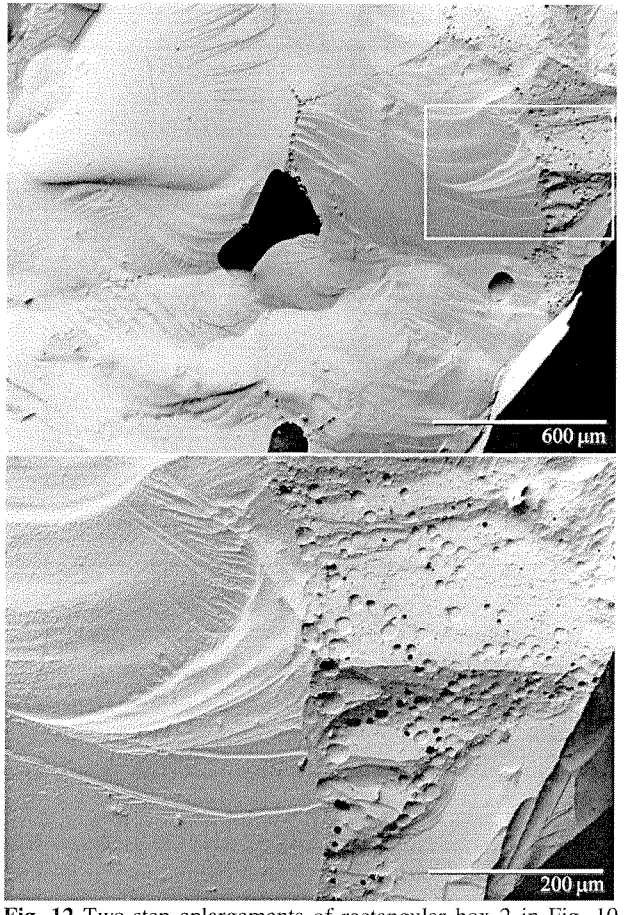

Fig. 12 Two-step enlargements of rectangular box 2 in Fig. 10, which shows numerous grain boundaries marked by small bubbles.

Both enlargements show features on the interior surface of the bubble and material that appears to be mineral particulates adhering to the ice. Paterson (1975) shows that individual glacier ice crystals can be seen by transmitting polarized light through thin ice sections and the crystals range in size from 2 mm to 15 mm. While the 8 mm corer precludes sampling of larger crystals, the SEM images show interesting structures in the glacier ice at scales of 2 mm and less. Figure 12 is another two-step enlargement of box 2 in Fig. 10, and it clearly shows what appear to be grain boundaries between individual ice crystals that have a scale of 1–2 mm. Lines of small bubbles define boundaries between crystals. The region of small bubbles on the right side of the lower panel in Fig. 12 shows the structure of what could be the surface between two crystals.

Figure 13 compares low-temperature SEM and video light microscope images of the identical glacier ice core taken approximately 8 cm below the dirty layer from SP-1841. Many more features are evident in the low-temperature SEM image than in light microscope image. Surface features such as boundaries of individual ice grains and adjacent pore spaces are clear using the SEM, whereas refraction, reflection, and diffusion of light within the ice core give poor resolution of the structure of the bulk

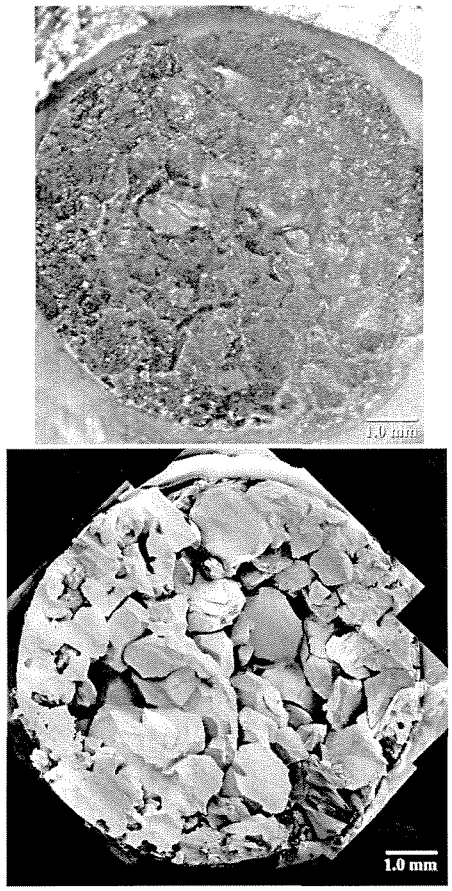

Fig. 13 SEM micrograph composite of identical core samples from 8 cm below the dirty ice layer at site SP-1841, imaged with a video light microscope (above) and the low-temperature SEM (below).

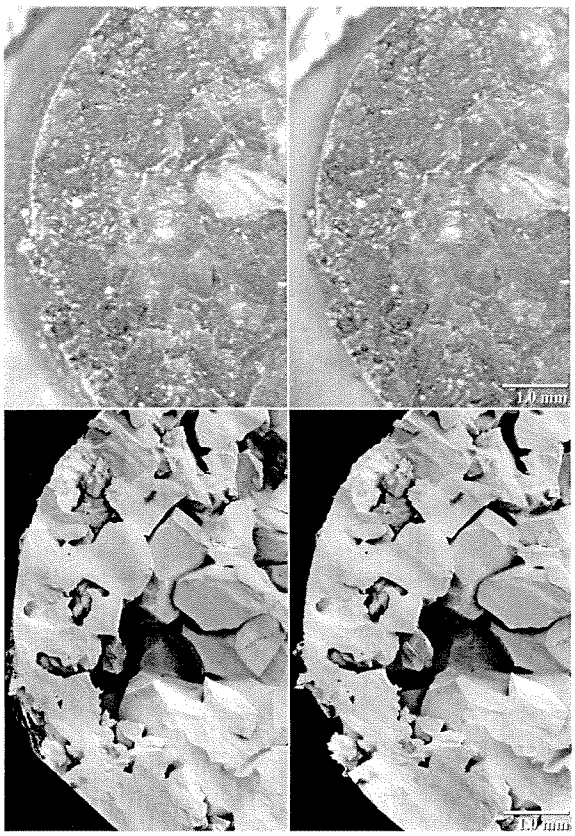

Fig. 14 Stereo micrograph pairs of a portion of the core illustrated in Fig. 13. In the light micrograph, (the top pair), the topography of the surface is more clearly apparent. The SEM micrographs (the bottom pair) clearly show the individual crystals and the connected air pockets. Boundaries of individual ice grains can easily be resolved. A three-dimensional (3-D) view of these stereo pairs can be obtained either by the unaided eyes or with the help of a simple lens viewer by entraining the left and right eyes on the left and right micrographs, respectively. When viewed in this manner, three images will be seen; the centre image will be the 3-D view that results from cortical fusion.

sample of the glacier ice using light microscopy. Figure 14 consists of stereo pairs of the left side of Fig. 13 for both types of images. Whereas the stereo views help distinguish features in the light micrograph, the stereo SEM image dramatically shows a 3-D view of the ice crystals, their association with adjacent crystals, and grain boundaries between adjacent crystals. The SEM methods can be used to quantify three-dimensional size, shape, and bonding characteristics of the ice crystals. The additional magnification possible with the SEM allowed detailed observation of boundaries between adjacent ice crystals.

While at the glacier, not only were snow and ice samples collected, but also samples of biota that are indigenous to mountain snowpacks and glaciers. Figure 15 is a low-temperature SEM of the "red" snow collected from the surface of the snowpack near the USGS hut. The algae are green algae, *Chlamydomonas nivalis*, and the cells are of the order of 10–15 μm in diameter as shown in the enlargement in the lower half

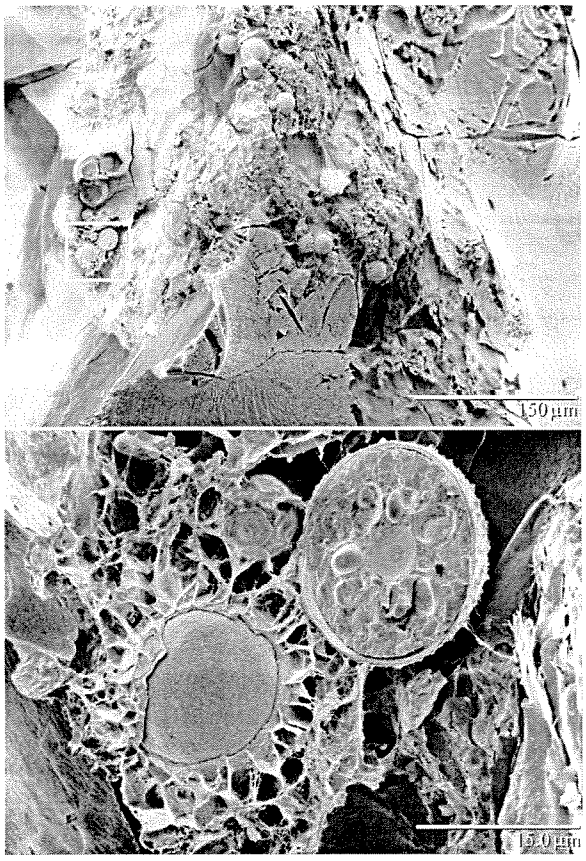

Fig. 15 Sample of red snow (containing green algae cells, *Chlamydomonas nivalis*) taken from snowfield surface near the glacier and imaged with the SEM. The upper panel shows numerous cells and the lower panel an enlarged view of two individual cells.

of Fig. 15. On the glacier samples of ice worms, a species of oligochaetes, were observed and collected. Figure 16 shows one of the ice worms collected from the snow pit at SP-1841. They measured 6–16 mm in length and about 0.5 mm in diameter and were dark brown or black in colour. The worms can move rapidly through the snow grains, and they feed on algae and other detritus in the snow on the glacier. They can be quite abundant on this and other glaciers in the temperate, maritime climate of the North Pacific Coast (Post & LaChapelle, 1971), sometimes reducing the albedo by as much as 5%. Generally, these worms appear on the surface when the energy balance is positive, but not in direct sunlight, and rapidly disappear when it is negative.

CONCLUSIONS

In Rango *et al.* (1996a), low temperature SEM was shown to solve many of the problems of photomicrography and photomacrography for imaging precipitated snow crystals. Rango *et al.* (1996b) showed that the techniques could be used in the field to

Fig. 16 Low temperature SEM image of an ice worm (a species of oligochaetes) which was collected 1m below the top of the seasonal snowpack at site SP-1841.

investigate a seasonal snowpack and provide images of metamorphosed snow crystals. Because glaciers have a very important influence on the hydrological cycle, it is necessary to understand both micro and macro processes in glacier hydrology. This study has shown that the techniques developed by Wergin *et al.* (1995a) can be used on remote glaciers. Samples of glacial ice types and biota associated with glaciers, can be obtained and shipped frozen at liquid nitrogen temperatures to the laboratory in Beltsville, Maryland for low-temperature SEM imaging and analysis.

Analysis of the images of snow, ice, and biota samples obtained from South Cascade Glacier shows that the SEM approach provides unique imaging capabilities to observe glacier ice. A comparison of SEM images with light microscope images of the same samples shows that the clarity and resolution of the SEM images is superior. This results from the fact that SEM images are derived only from surface features, whereas the light microscope images are made up of a combination of reflection, refraction, and diffusion of light within the ice or snow sample. The resolution of SEM images of snow and ice is several orders of magnitude improved over light microscopy for ice crystal structural analysis. Boundaries between glacier ice crystals and features on the surface of the crystals are much easier to detect with the SEM technique. From studies of the SEM glacier ice crystals, it is common to see microscopic gas volumes (bubbles of about 15 μm diameter or less) aligned along ice grain boundaries. The substructure

of these bubbles (faceting and mineral particulates contained within the bubbles) can also be seen. The resulting images of firn show individual ice crystals, bonding between the crystals, and interconnected air spaces. Images of glacier ice show a crystal dimension of 1–2 mm which is considerably smaller than the 2–15 mm range cited by Paterson (1975). Algae cells that have been detected in snowpacks from other areas are also present on the South Cascade Glacier. These algae cells can be imaged by SEM at better resolution than by any other means. In addition, the presence of ice worms on South Cascade Glacier and their shape and form has been documented in a way not previously possible.

The SEM approach to obtaining snow and ice photomicroscopy can provide a large number of photos in a short period of time. In less than four years of part time instrument usage, more than 15 000 photos of snow and ice samples have been produced, documenting a wide variety of ice types. Although the cost of the actual SEM is high, it must be recognized that snow and ice studies are only one of a large number of applications for the SEM. The large number of samples that can be processed in a room temperature laboratory, the indefinite preservation of samples, and the much clearer images, combine to make the SEM approach cost effective when compared with traditional light microscopy.

Acknowledgements The authors thank Robert Krimmel, USGS, for stimulating discussions concerning glacier firn and its distribution on South Cascade Glacier.

REFERENCES

Ahlmann, H. W. & Droessler, E. C. (1949) Glacier ice crystal measurements at Kebnekajse, Sweden. *J. Glaciol.* **1**(8).

Aizen, V. B., Aizen, E. M. & Melach, J. M. (1996) Precipitation, melt, and runoff in the northern Tien Shan. *J. Hydrol.* **186**, 229–251.

Eckerbom, E. & Palosuo, E. (1963) A study of ice at Storglaciaren, Kebnekajse. In: *Ice and Snow: Properties, Processes, and Applications* (ed. by W. D. Kingery), 56–62. MIT Press, Cambridge, Massachusetts, USA.

Foster, J. L. & Rango, A. (1982) Snow cover conditions in the northern hemisphere during the winter of 1981. *Int. J. Clim.* **20**, 171–183.

Hall, D. K. & Martinec, J. (1985) *Remote Sensing of Ice and Snow.* Chapman and Hall, New York, USA.

Hodge, S. M., Trabant, T. C., Krimmel, R. M., Heinrichs, T. A., March, R. S. & Josberger, E. G. (1998) Climate variations and changes in mass of three glaciers in western North America. *J. Climate* **11**(9), 2161–2179.

Krimmel, R. (1993) Mass balance, meteorological and runoff measurements at South Cascade Glacier, Washington, 1992 balance year. US Geol. Survey Wat. Resour. Investigations Report no. 93–640, Tacoma, Washington, USA.

Krimmel, R. (1994) Runoff, precipitation, mass balance and ice velocity measurements at South Cascade Glacier, Washington, 1993 balance year. US Geol. Survey Wat. Resour. Investigations Report no. 94–4139, Tacoma, Washington, USA.

Krimmel, R. (1995) Water, ice, and meteorological measurements at South Cascade Glacier, Washington, 1994 balance year. US Geol. Survey Wat. Resour. Investigations Report no. 95–4162, Tacoma, Washington, USA.

Krimmel, R. (1996) Water, ice, and meteorological measurements at South Cascade Glacier, Washington, 1995 balance year. US Geol. Survey Wat. Resour. Investigations Report no. 96–4174, Tacoma, Washington, USA.

Meier, M. F., Tangborn, W. V., Mayo, L. R., & Post, A. (1971) Combined ice and water balances of Gulkana and Wolverine Glaciers, Alaska, and South Cascade Glacier, Washington, 1965 and 1966 water years. US Geol. Survey Prof. Paper no. 715–A.

Ostrem, G. (1972) Runoff forecasts for highly glacierized basins. In: *The Role of Snow and Ice in Hydrology* (Proc. Banff Symp., September 1972), 1111–1132. IAHS Publ. no. 107.

Paterson, W. S. B. (1975) *The Physics of Glaciers.* Pergamon Press, New York, USA.

Post, A. & LaChapelle, E. R. (1971) *Glacier Ice.* The Mountaineers/The University of Washington Press, Seattle.

Post, A. P., Richardson, D., Tangborn, W. V. & Rosselet, F. L. (1971) Inventory of glaciers in the North Cascades. US Geol. Survey Prof. Paper no. 705A.

Rango, A., Wergin, W. P. & Erbe, E. F. (1996a) Snow crystal imaging using scanning electron microscopy: I. Precipitated snow. *Hydrol. Sci. J.* **41**(2), 219–233.

Rango, A., Wergin, W. P. & Erbe, E. F. (1996b) Snow crystal imaging using scanning electron microscopy: II. Metamorphosed snow. *Hydrol. Sci. J.* **41**(2), 235–250.

Richardson, D. (1972) Effect of snow and ice on runoff at Mount Ranier, Washington. In: *The Role of Snow and Ice in Hydrology* (Proc. Banff Symp., September 1972), 1172–1185. IAHS Publ. no. 107.

Seligman, G. (1949) The growth of the glacier crystal. *J. Glaciol.* **1**(5), 254–268

Wergin, W. P. & Erbe, E. F. (1994a) Can you image a snowflake with an SEM? Certainly! *Proc. Royal Microsc. Soc.* **29**, 138–140.

Wergin, W. P. & Erbe, E. F. (1994b) Snow crystals: Capturing snowflakes for observation with the low temperature scanning electron microscope. *Scanning* **16**, IV88–IV89.

Wergin, W. P. & Erbe, E. F. (1994c) Use of low temperature scanning electron microscopy to examine snow crystals. In: *Proc. 14th Int. Congress of Electron Microscopy* **3**(B), 993–994.

Wergin, W. P., Rango, A. & Erbe, E. F. (1995a) Observations of snow crystals using low-temperature scanning electron microscopy. *Scanning* **17**, 41–49.

Wergin, W. P., Rango, A. & Erbe, E. F. (1995b) Three dimensional characterization of snow crystals using low temperature scanning electron microscopy. *Scanning* **17**, V29–V30.

Wergin, W. P., Rango, A., Erbe, E. F. & Murphy, C. A. (1996) Low temperature SEM of precipitated and metamorphosed snow crystals collected and transported from remote sites. *J. Microscopy Soc. Am.* **2**(3), 99–112.

Wergin, W. P., Rango, A. & Erbe, E. F. (1998) Image comparisons of snow and ice crystals photographed by light (video) microscopy and low temperature scanning electron microscopy. *Scanning* **20**, 285–296.

Received 8 September 1998; accepted 7 February 2000